Numerical Analysis of Bending Toughness of Steel Fiber Reinforced Cement Based Materials

Yunguo Zhang, Suning Li, Tingting Zhu, Gang Li

School of Civil Engineering, Dalian Jiaotong University, Dalian 116028, Liaoning, China

Abstract. Steel fibers have a significant toughening effect on cement-based materials. In order to address the issue of relying solely on experimental evaluation of their bending toughness, a numerical analysis method based on the steel fiber bridging theory has been proposed. By establishing a crack extension criterion for fiber-reinforced cement-based composite materials based on the balance between the stress intensity factor generated by external loads, steel fibers, and matrix cohesion at the crack tip and the fracture toughness of the composite material, the toughness of the composite material is evaluated. Through steel fiber-matrix pull-out tests, the bonding characteristics of four types of steel fibers, namely shear, milling, short hook, and long hook, with the matrix are analyzed. A program is then developed using Ansys software APDL language for numerical simulation of the bending and cracking process of the notched beam of the steel fiber-reinforced cement-based composite material. The obtained load-deflection curve and bending toughness index are compared with the results of the notched beam bending test, thereby validating the correctness of the numerical analysis method. The results show that the bending toughness of steel fiber-reinforced cement-based composite materials is closely related to the volume fraction of steel fibers and their bonding characteristics. The balance relationship of the stress intensity factor at the crack tip is the key factor determining crack propagation, and the proposed numerical analysis method can effectively assist in the analysis of the bending toughness of steel fiber-reinforced cement-based composite materials.

Keywords: Steel fibers, cement-based composite materials, numerical analysis, pull-out test, bending toughness, crack propagation

1. Introduction

With the rapid development of engineering technology, new and higher requirements have been placed on materials for 3D printing, prefabricated structures, and other applications. In general, cement-based materials have the drawback of low tensile strength and poor toughness. However, adding steel fibers to the material can prevent microcracks in the cement matrix from expanding and deteriorating before cracking, and can also bridge macrocracks after cracking, bearing tensile stress and hindering their development. Steel fiber-reinforced cement-based composites, composed of cement slurry, mortar or cement concrete as the matrix material and non-continuous short fibers or continuous long fibers as the reinforcement material, have excellent characteristics such as tensile strength, bending resistance, impact resistance, and high toughness, and have been widely used in various fields of civil engineering.

Due to the heterogeneity and complexity of steel fiber reinforced cement-based composites, a combined approach of experimental and theoretical research is typically employed to investigate their mechanical and other properties. Kazim et al. [1] studied the effect of fiber volume fraction and combination on the flexural performance of fiber-reinforced concrete with mixed long and thin fibers and short and thick fibers through experimental research. Kang et al. [2] evaluated the influence of pouring direction and fiber distribution characteristics on the bending strength of composite materials. Silva et al. [3] demonstrated through experimentation that steel fibers have a significant toughening effect on cement-based materials, and that both flexural strength and toughness increase with increasing fiber length.

Flexural toughness is used to evaluate the toughening effect of high-strength and high-ductility fiber materials on cement-based materials after cracking, and is generally calculated and analyzed based on the energy absorbed by concrete during the flexural failure process [4]. The flexural toughness test method can effectively analyze the actual stress conditions of most engineering components, making flexural toughness the most commonly used indicator to measure the quality of steel fiber reinforced composites [5]. Banthia et al. [6] studied the toughness of curled fiber concrete using the ASTM flexural toughness evaluation method. Smarzewski [7] conducted three-point bending tests on notched beams and unnotched specimens, and calculated and compared the toughness using evaluation methods such as ASTM and RILEM. Dong et al. [8] investigated the flexural toughness of ultrafine steel fiber reinforced concrete and established a flexural toughness model based on composite material theory.

In summary, the bending toughness of steel fiber reinforced cement-based composites is influenced by various factors, and can be studied through different bending toughness test and evaluation methods. However, while testing can quantitatively evaluate the toughening effect of steel fibers on cement-based materials, the results have a large degree of variability due to issues with specimen preparation and testing methods. Therefore, this paper proposes a crack propagation criterion, whereby the bonding characteristics between the matrix and steel fibers are determined via fiber pullout testing. Finite element numerical analysis is then used to simulate the bending crack process of the notched beam of steel fiber reinforced cementitious composites and verified through experimentation, allowing for the analysis of the bending crack process of fiber composite materials and providing theoretical and practical basis for the study of the bending toughness of fiber-reinforced cement-based composites.

2. Experimental procedure

2.1. Raw materials

The experiment used P·O 42.5R ordinary Portland cement. The fine aggregate used was river sand, with an apparent density of 2650 kg/m3 and a fineness modulus of 2.79. A polycarboxylate-based high-efficiency water reducing agent was used, with a solid content of 24.02% and a water reduction rate greater than 28%. Grade I fly ash was used as an additive, with a loss on ignition of 2.62%. The water-cement ratio of the composite material was 0.36, the sand ratio was 0.41, and the replacement rate of fly ash was 30%. The unit volume of materials used is shown in Table 1. The average compressive strength of the cubes at 28 days was measured to be 41.34 MPa, the elastic modulus was 32.0 GPa, and the Poisson's ratio was 0.2. All specimens were made with the same raw materials.

Table 1 Mix Proportions for Matrix

Material	Volume Ratio	Mass (kg/m^3)
Cement	0.26	579.5
Fly ash	0.11	248.4
River sand	0.5	1086.5
Water	0.13	298
Water-reducing agent	0.002	4.9

To comprehensively investigate the influence of different types of steel fibers on toughness enhancement, four types of steel fibers, including shear-type, milling-type, hooked-end short-type, and hooked-end long-type. The detailed parameters of the steel fibers are listed in Table 2.

Table 2 Physical Properties of Steel Fibers

Physical Properties	F1	F2	F3	F4
Fiber Type	Shear Type	Milling Type	Short Hook Type	Long Hook Type
Cross-Sectional Shape	Crescent-shaped	Rectangle	Circular	Circular
Average Length/mm	38	38	35	60
Equivalent Diameter/mm	0.596	0.952	0.75	0.75
Tensile Strength/MPa	400	700	1100	1100
Aspect Ratio	63.8	40	46.7	80
Figure legend				

2.2. Tensile test

The steel fiber pull-out test was conducted following the recommended method in the "Standard Test Methods for Fiber-Reinforced Concrete" [9] (CECS13-2009). The test specimens were cast using an 8-shaped metal mold that meets the standard specifications. A 1mm thick PVC plate was used to separate the minimum interface in the middle of the mold, with four small circular holes (15mm apart) for placing steel fibers. During the assembly of the mold, it was ensured that the mold remained undistorted and did not leak water. The partition was placed vertically in the mold and a release agent was applied to the inner surface of the mold and the partition. The steel fibers were inserted into the circular holes and fixed with universal glue to keep them perpendicular to the partition. The pull-out test machine was driven by a servo motor, and the loading process was achieved by driving the cantilever to move up and down through a transmission mechanism. The expected failure load of the test specimen was between 20% and 80% of the full scale, with an accuracy of not less than 1%. The load-displacement curve of the pull-out process was obtained by connecting the load sensor and displacement sensor to the DH5922 data acquisition instrument. The specimens were continuously and uniformly loaded at a loading rate of 0.3mm/min. When the steel fibers slipped more than 6mm, the loading was stopped. The loading process of the pull-out test is shown in Figure 1.

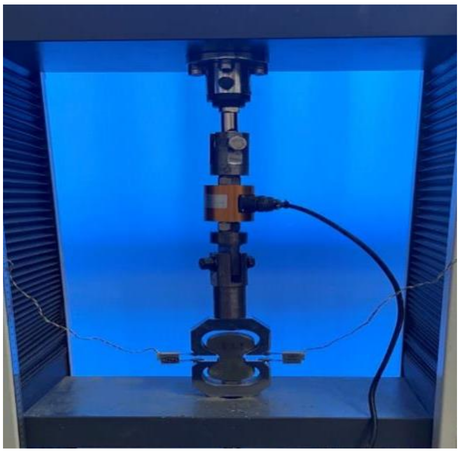

Fig. 1 Load diagram of a tensile testing machine

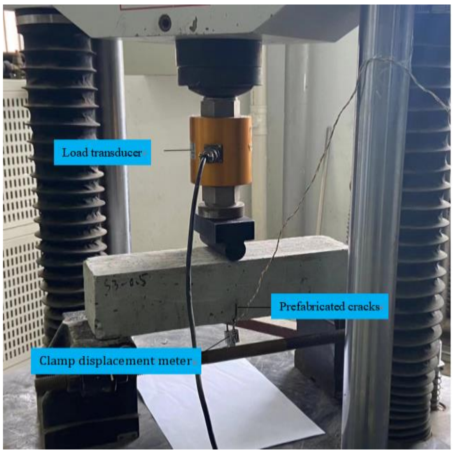

Fig. 2 Schematic diagram of bending toughness test

2.3. Bend toughness test

The bend toughness test is conducted using a three-point bending notched beam, with a pre-existing crack perpendicular to the bottom surface and a slit width of 2mm. The mixture ratio of the specimens is identical to that used for the tensile test, as shown in Table 1. Four types of steel fibers (F1, F2, F3, F4) are selected with their material properties listed in Table 2. Each steel fiber type is mixed at two different dosages, namely, a lower dosage of 0.5% and a higher dosage of 1.5%. The grouping of the specimens is presented in Table 3, with a total of eight groups. After being kept in a curing room for 28 days according to standard procedures, the specimens are ready for testing.

Table 3 Grouping of specimens for bend toughness test

Sample ID	Fiber Type	Fiber Dosage(%)	Fiber Length (mm)
LF105	F1	0.5	38
LF205	F2	0.5	38
LF305	F3	0.5	35
LF405	F4	0.5	60
LF115	F1	1.5	38
LF215	F2	1.5	38
LF315	F3	1.5	35
LF415	F4	1.5	60

The three-point bending test is performed on a computer-controlled hydraulic servo universal material testing machine. The support restraint is placed 25mm away from the edge of the specimen model. The crack opening displacement is measured using a displacement extensometer clamped at the bottom of the pre-notched beam. The load value is recorded using a load sensor. The loading rate is set to 0.2mm/min. Figure 3 illustrates the loading process of the pre-notched beam in the three-point bending test.

3. Numerical simulation of the bending cracking process

3.1. The establishment of the finite element model

Using Ansys software, we simulated and analyzed the bending and cracking process of a notched beam, and established a two-dimensional finite element model of a simply supported beam with dimensions of 400mm (length) x 100mm (width) x 100mm (height) according to the bending toughness test plan. The PLANE82 element with 6 nodes per triangle was used to discretize the model. To make the numerical simulation more consistent with the actual test conditions, we processed the notched specimen by creating two overlapping straight lines with the upper end point of the overlapping line as the vertex of the notch, and the length of the overlapping part as the length of the notch, which was 25mm. The distance between the two support points was 350mm.

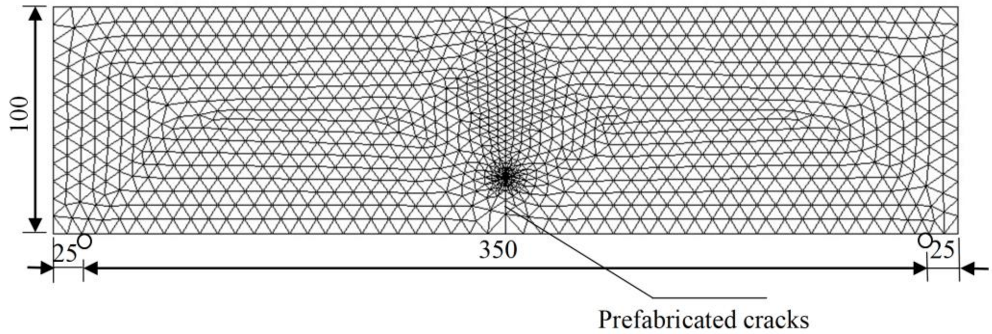

Fig. 3 Mesh model partitioning

3.2. Constitutive relation

The material constitutive relation used in finite element analysis has a significant impact on the accuracy of numerical simulations. In the numerical simulation of the bending and cracking of notched beams, Reinhardt's proposed nonlinear softening constitutive relation curve is used to calculate the constitutive model of the cement matrix [10], as shown in equation (1):

$$\frac{\sigma_m}{f_t}=[1+(c_1\frac{\omega}{\omega_c})^3]e^{-c_2\frac{\omega}{\omega_c}}-\frac{\omega}{\omega_c}(1+c_1^3)e^{-c_2} \tag{1}$$

Where σ_m is the crack cohesion, ω is the crack opening displacement, f_t is the tensile strength of plain concrete, c_1 and c_2 is a material dependent constant, the width of the crack when ω_c is $\sigma_m=0$, $f_t=2.4\text{MPa}$, $c_1=3$, $c_2=6.93$, $\omega_c=0.16\text{mm}$ in analysis.

The constitutive relationship used for cracks inside composite materials is based on the bridging stress and crack opening displacement model related to fiber bonding [11], In cement matrix, the fiber undergoes two stages of debonding and slipping when it is subjected to external tension. The debonding stage is expressed as:

$$\sigma_{f1}(\omega)=\frac{\tau V_f L_f \xi\theta}{2d_f}(2\sqrt{\frac{\omega}{\omega_0}}-\frac{\omega}{\omega_0}), \quad (\omega<\omega_0) \tag{2}$$

Where σ_{f1} is the bridging stress during the debonding process of steel fibers, τ is the bond strength between steel fiber and substrate during the drawing process, and it can be determined through experiments., ξ is the chemical bonding between steel fibers and matrix. However, as the experimental material in this study is steel fibers, the chemical bonding effect can be neglected. V_f is the steel fiber volume fraction., and d_f is the diameter of steel fibers, The parameter θ denotes the distribution of steel fibers, and in this case, its value is 2.

Once the fiber is fully debonded, the interfacial adhesion between the fiber and matrix primarily depends on physical friction. The equation for fiber slip can be expressed as follows:

$$\sigma_{f2}(\omega)=\frac{\tau V_f L_f \xi\theta}{2d_f}(1-2\omega/L_f)^2, \quad (\omega_0<\omega<L_f/2) \tag{3}$$

Where σ_{f2} is the bridging stress during the slip process of steel fibers.

3.3. Crack propagation criteria

When SFRC cracks are regarded as homogeneous materials on a macro scale, based on the crack initiation toughness expansion criterion [12], the fiber concrete expansion criterion is proposed. When the crack initiation toughness K^{ini} of steel fiber concrete is achieved by superposing the crack tip stress intensity factor K^{σ} caused by the cohesion of concrete matrix, the crack tip stress intensity factor K^{P} caused by external load P and the fiber bridging stress intensity factor K^{f} , the cracks begin to expand, namely:

$$K^{P} + K^{\sigma} + K^{f} = K^{ini} \tag{4}$$

All these stress intensity factors can be solved by finite element method. In the propagation of cracks, the following conditions will occur:

(1) When $K^{P} + K^{\sigma} + K^{f} < K^{ini}$ occurs, it is because of excessive cohesion that the load continues to increase and the crack does not propagate.

(2) When $K^{P} + K^{\sigma} + K^{f} = K^{ini}$, the torque generated by the external load is in relative balance with the force within the crack, and the crack will expand steadily forward.

(3) When $K^{P} + K^{\sigma} + K^{f} > K^{ini}$, the cohesion is reduced and the load is reduced to maintain the new equilibrium and continue to expand steadily forward.

According to the above crack propagation criterion, the stress intensity factor $K^{P} + K^{\sigma} + K^{f}$ and crack initiation toughness K^{ini} are compared to determine the increase or decrease of load. When the superposition value is equal to the fracture toughness, the original fracture is extended forward by a small increment. Repeat the process until the specimen is completely destroyed.

4. Experimental verification and analysis

4.1. Experimental Results and Discussion

By conducting experiments, the maximum load and displacement at which steel fibers are pulled out can be obtained as $F_{\max}$ and w_0 , respectively. The interfacial bond strength between steel fibers and cement mortar is calculated as τ_0 . The maximum load capacity of each type of steel fiber and their bond strength of τ_0 are summarized in Table 4.

Table 4 Drawing test results of steel fiber

ID	$F_{\max}$(N)	w_0(mm)	τ_0(MPa)
F1	2168.7	2.596	8.183
F2	1889.5	1.55	4.335
F3	1114.4	1.252	3.505
F4	1779.7	2.721	3.298

The experimental results indicate that the surface shape and aspect ratio of steel fibers of different types can significantly influence the interfacial bonding performance between steel fibers and cement-based materials. Comparing two types of steel fibers, F1 and F2, with the same average length, at the same burial depth, the different cross-sectional shapes result in varying contact surface areas and angles between cement mortar and steel fibers. Under external forces, the contact surface changes continuously as the steel fiber is pulled out, leading to completely different interfacial bond strengths between the steel fiber and cement mortar. Comparing two types of steel fibers, F3 and F4, with the same cross-sectional shape, the burial depth of F4 is higher than that of F3. As the fiber burial depth increases, the ultimate pullout force also increases, but so does the displacement at maximum load. As a result, the difference in interfacial bond strength is not significant. Therefore, it can be concluded that increasing fiber length can increase the pullout force between cement mortar and steel fibers, but the main factor affecting interfacial bond strength is the different cross-sectional shapes of the steel fibers.

4.2. Comparison of Load-Deflection Curves

During the loading process of the experiment, when the load reached the initial cracking load, cracks appeared at the notch at the bottom of the specimen. The load continued to increase, and the mid-span deflection also increased continuously, while the cracks gradually extended towards the loading point. After the loading was stopped, most of the steel fibers remained closely connected to the concrete matrix, and only a few fibers were pulled out at the cracked locations, with almost no broken steel fibers.

Figure 8 shows the complete load-deflection curves for the notched beam specimens of steel fiber reinforced concrete during bending, both in experiment and simulation. From the figure, it can be observed that after reaching the first peak load at low fiber volume fractions, there is a significant drop in the load-deflection curves for all four types of steel fibers. This is due to the weak bond between the steel fibers and the matrix at low fiber volume fractions. As the deflection increases, cracks propagate forward, and more steel fibers participate in the crack bridging process. As a result, some of the load-deflection curves for the steel fiber reinforced concrete show a varying degree of upward trend and then gradually decrease after reaching the second peak load until stabilizing. On the other hand, at high fiber volume fractions, the load-deflection curves for the steel fiber reinforced concrete decrease slowly after reaching the peak load due to the strong bond between the steel fibers and the concrete matrix.

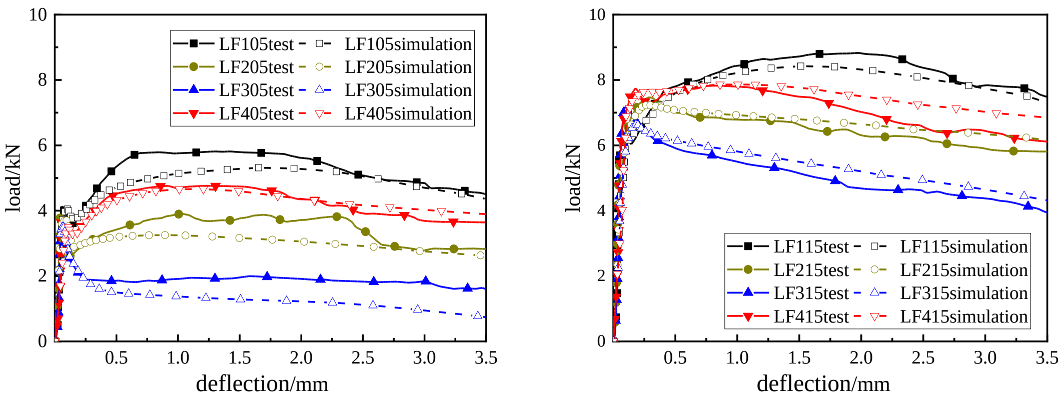

a. Load deflection curve of steel fiber concrete with low content

b. Load deflection curve of steel fiber concrete with high content

Fig. 4 Test and simulation of load deflection curves of notched beam specimens during bending

Upon comparing the numerical simulation and experimental results, the overall trend of the numerical simulation's load-deflection curve agrees well with that of the experimental results. However, the residual load of the numerical simulation after the peak load of the load-deflection curve is generally lower than the experimental values. This is mainly due to the fact that the finite element model's interface bonding strength stress intensity factor is smaller than the experimental model because the effect of steel fiber shape on bonding is not considered in the constitutive relationship of the finite element model during the relative slip process between the steel fibers and the concrete matrix.

Due to the nonlinearity of the ascending segment of the load-deflection curve, it is difficult to accurately determine the location of the initial cracking point. However, comparing the simulation results with the experimental results shows a maximum error of 8.601% and an average error of 4.803%. Analysis shows that the numerical simulation method is reliable and effective, as the simulated values are close to the experimental values.

4.3. Comparison of Flexural Toughness Indicators

In reference to the JSCE SF4 flexural toughness evaluation method [13] established by the Japan Society of Civil Engineers, a comparison of flexural toughness indicators is made between the above test results and simulation results. The JSCE SF4 flexural toughness evaluation method uses the equivalent flexural strength fs as the evaluation indicator, which is calculated using the following formula:

$$f_s = \frac{L}{BH^2} \cdot \frac{T_k}{\delta_k} \tag{5}$$

In this equation, δ_k refers to the set vertical deflection value, which is taken as $L/150$ according to JSCE SF4. L is the span between the two supports, while H and B are the height and width of the specimen, respectively. T_k represents the area enclosed by the load-deflection curve at the deflection value of δ_k .

Using the JSCE SF4 bending toughness evaluation method, the bending toughness index for the experimental and simulated results is shown in Figure 5.

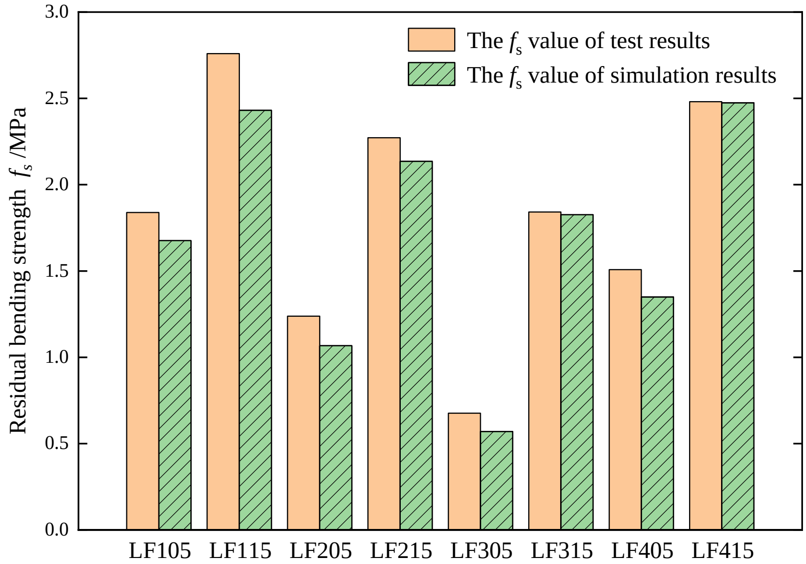

Fig. 5 Comparison of bending toughness indexes of JSCE SF4

During the comparison of the bending toughness indicators using the JSCE SF4 bending toughness evaluation method, the maximum error was found to be 15.68% and the average error was 8.49%. The small difference between the numerical simulation and experimental results confirmed the accuracy of the simulation process. For the same type of steel fiber, the equivalent bending strength fs of high-dose steel fiber reinforced concrete was higher than that of low-dose steel fiber reinforced concrete. However, for different types of steel fiber, the difference in equivalent bending strength for the same dosage was significant. For example, the equivalent bending strength of F3-type steel fiber reinforced concrete with a 0.5% dosage was only slightly higher than that of F1-type steel fiber reinforced concrete with a 1.5% dosage, indicating that the fiber type is one of the main factors affecting the bending toughness of steel fiber reinforced cementitious composites.

5. Conclusion

In this study, tensile tests were performed on different types of steel fibers, and the bonding parameters obtained from the tests were used to simulate the flexural performance of steel fiber reinforced cement-based composites using numerical simulation. The simulation results were compared with the load-deflection curve and flexural toughness index obtained through bending tests, and the following conclusions were drawn:

(1) By comparing the load-deflection curve and flexural toughness index of the structure with the experimental data, it is proved that the numerical simulation method is reliable and effective.

(2) The type of fiber can greatly influence the bonding performance between steel fibers and cement-based materials, and thus affect the flexural performance of steel fiber reinforced cement-based composites. The main factor affecting the interfacial bond strength is the different cross-sectional shapes of steel fibers. When the fiber type is the same, increasing the fiber content significantly improves the toughness of steel fiber reinforced cement-based composites.

(3) Flexural toughness can effectively reflect the toughening performance of steel fibers. The accuracy of the numerical simulation results of steel fiber reinforced cement-based composites can be verified by comparing the flexural toughness index. The JSCE SF4 bending toughness evaluation method can calculate the flexural toughness of the entire load-deflection curve.

Declaration of Competing Interest

The author declares that there is no conflict of interest in relation to this manuscript.

Acknowledgements

This work was financially supported by the Foundation of Liaoning Education Department of China (LJKZ0498). The authors acknowledge Dalian Huanqiu Minerals Co., Ltd. for the test materials.

References

[1] Kt A, Mb B, Reb C. Workability, strength and flexural toughness properties of hybrid steel fiber reinforced SCC with high-volume fiber [J]. Construction and Building Materials, 266.

[2] Su T K, Bang Y L, Kim J K, et al. The effect of fibre distribution characteristics on the flexural strength of steel fibre-reinforced ultra-high strength concrete [J]. Construction & Building Materials, 2011, 25(5): p.2450-2457.

[3] Silva G, Christ R, Pacheco F, et al. Evaluating steel fiber - reinforced self - consolidating concrete performance [J]. Structural Concrete, 2020.

[4] Han Jianguo, Yan Peiyu. A review of testing and evaluation methods for flexural toughness of concrete [J]. 2022(11).

[5] Gao Dan-ying, Zhao Liang-ping, Feng Hu, et al. Flexural toughness of steel fiber reinforced concrete and its evaluation method [J]. Journal of Building Materials, 2014, 17(5):7.

[6] Banthia N, Sappakittipakorn M. Toughness enhancement in steel fiber reinforced concrete through fiber hybridization [J]. Cement & Concrete Research, 2007, 37(9):1366-1372.

[7] Smarzewski P. Flexural toughness evaluation of basalt fibre reinforced HPC beams with and without initial notch [J]. Composite Structures, 2019, 235:111769.

[8] Dong S, Zhou D, Ashour A, et al. Flexural toughness and calculation model of super-fine stainless wire reinforced reactive powder concrete [J]. Cement and Concrete Composites, 2019, 104:103367-.

[9] Dalian University of Technology. Test Method Standard for fiber Concrete: CECS-13 2009 [S]. Beijing, China Planning Press,2010.

[10] Reinhardt H W, Cornelissen H, Hordijk D A. Tensile Tests and Failure Analysis of Concrete [J]. Journal of Structural Engineering, 1986, 112(11):2462-2477.

[11] Li C, Victor. Postcrack Scaling Relations for Fiber Reinforced Cementitious Composites [J]. Journal of Materials in Civil Engineering, 1992, 4(1):41-57.

[12] Xu Shiliang, Zhao Yanhua. Fracture Theory and Analysis method of concrete Crack Propagation [C]// Proceedings of the 17th National Conference on Structural Engineering (Vol.1). 2008.

[13] Institute J C. Test methods for flexural strength and toughness of fiber reinforced concrete [J]. JCI-SF4, 1984.